Acta Crystallographica Section D
Biological Crystallography
ISSN 0907-4449

Structure of the side-by-side binding of distamycin to d(GTATATAC)$_2$

Shome Nath Mitra, Markus C. Wahl and Muttaiya Sundaralingam*

The Ohio State University, Biological Macromolecular Structure Center, Departments of Chemistry and Biochemistry, 012 Rightmire Hall, 1060 Carmack Road, Columbus, Ohio 43210-1002, USA

Correspondence e-mail: sundaral@chemistry.ohio-state.edu

Received 19 June 1998
Accepted 28 September 1998

PDB Reference: distamycin–d(GTATATAC)$_2$, gdh060.

The 2.40 Å resolution crystal structure of a side-by-side binding of distamycin A molecules to a DNA octamer d(GTATATAC)$_2$ with an extended alternating TA sequence has been determined. The unit-cell parameters are a = 29.55, b = 42.18, c = 43.38 Å, β = 96.56°, space group $P2_1$, with two molecules in the asymmetric unit, in contrast to all previous side-by-side distamycin–DNA complexes which have only a single DNA strand and one drug molecule in the asymmetric unit. The structure was solved by the molecular-replacement method and refined to an R index of 21.0% using 3467 reflections [$\geq 2\sigma(F)$]. The minor grooves of the DNA molecules bind two side-by-side antiparallel staggered distamycins spanning about five base pairs and virtually covering the entire length of the DNA. The octamer duplexes exhibit low–high alternations in the helical twist, sugar puckering and the C—O3′ and O3′—P torsion angles, similar to the earlier side-by-side complexes containing inosine bases. The molecules are stacked one over the other along the *ac* diagonal in an infinite pseudo-continuous helical column with no lateral interactions.

1. Introduction

Minor-groove binding drugs prevent the *in vitro* synthesis of DNA and RNA by inhibiting the corresponding polymerase reaction through their interaction with the DNA template (Wahnert *et al.*, 1975; Burckhardt *et al.*, 1989). Various drug–DNA complexes have been studied for 15 years as targets for designing effective antitumor agents. Studies have been conducted to gain a knowledge of the structure, the thermodynamics of complex formation and the binding specificity of minor-groove drugs (Wartell *et al.*, 1974; Zakrzewska *et al.*, 1983; Patel & Shapiro, 1985; Zimmer & Wahnert, 1986). The natural drugs netropsin and distamycin (Fig. 1) are known to bind to the minor groove of B-DNA with sequence specificity to A–T/I–C regions, while steric hindrance of the 2-amino group of G prevents the binding of these drugs to G–C base pairs (Wartell *et al.*, 1974). The crystal structure analysis of a 1:1 netropsin–d(CGCGAATT^{Br}CGCG) complex (Kopka *et al.*, 1985*a*) confirmed the binding specificity of netropsin to the A–T/T–A region of DNA and prompted other studies of minor groove drug–DNA complexes both in solution (Portugal & Waring, 1987) and in the solid state (Coll *et al.*, 1987; Wang & Teng, 1990; Kopka & Larsen, 1992). In the 1:1 complexes, the hydrogen bonding of the DNA strands to the drugs and van der Waals interactions between the sandwiching backbones play crucial roles in stabilizing the complexes. The synthetic lexitropsin drugs, in which the *N*-methyl pyrrole rings of netropsin are replaced by *N*-methyl imidazole rings

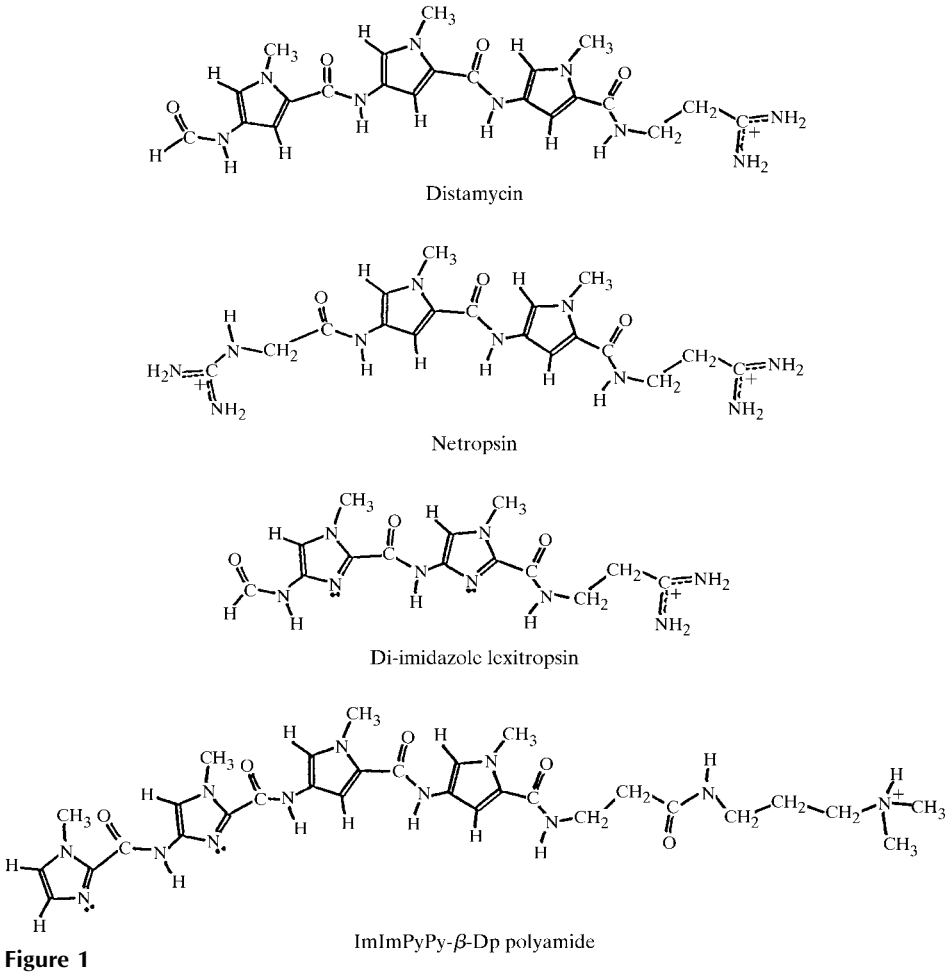

Figure 1
Molecular structure of distamycin, netropsin, di-imidazole lexitropsin and ImImPyPy-β-Dp polyamide (Im, *N*-methylimidazole carboxamide; Py, *N*-methyl pyrrole carboxamide; Dp, dimethylaminopropylamide).

(Fig. 1), were designed to recognize G–C base pairs specifically (Kopka *et al.*, 1985*a*,*b*; Lown *et al.*, 1986), but in the 1:1 binding mode indiscriminately bind to both G–C/C–G and A–T/T–A base pairs (Kopka & Larsen, 1992; Goodsell *et al.*, 1995). A major breakthrough came after the 2:1 side-by-side binding of distamycin was demonstrated by solution NMR (Pelton & Wemmer, 1989) and X-ray crystallography (Chen *et al.*, 1994). The side-by-side drug binding led to new design principles for recognition of G–C/C–G base pairs with sequence specificity (Mrksich & Dervan, 1993; Geierstanger *et al.*, 1994; Geierstanger & Wemmer, 1995) and provided sequence-reading rules for the imidazole–pyrrole pair, which can differentiate G–C from C–G (White *et al.*, 1997). In contrast, the pyrrole–pyrrole pair binds A–T and T–A indiscriminately, while the imidazole–imidazole pair appears to favor G–C/C–G pairs (White *et al.*, 1997; Kopka *et al.*, 1997). Indeed, the synthetic drug di-imidazole lexitropsin (Kopka *et al.*, 1997) and a pyrrole–imidazole polypeptide (Fig. 1) (Kielkopf *et al.*, 1998) differentiate G–C from C–G and also from A–T and T–A in this binding mode. Recently, a third ring, hydroxypyrrole, was added to break the A–T/T–A degeneracy (White *et al.*, 1998).

The work of Kopka *et al.* (1985*a*) inspired us to study more examples of crystal structures of various DNA sequences complexed to minor-groove binding drugs. We have previously reported the crystal structure of the 1:1 complex of netropsin and a DNA dodecamer d(CGCGTTAACGCG) (Balendiran & Sundaralingam, 1991; Balendiran *et al.*, 1995), the 2:1 side-by-side binding of distamycin to the DNA octamer with unnatural inosine bases d(ICICICIC) (Chen *et al.*, 1994), the same octamer with mixed ribose and deoxyribose sugars (IcICICIC) and (IcIcICIC), where c represents ribo-cytidine (Chen *et al.*, 1995), and with the central I–C base pairs replaced by A–T base pairs (Chen *et al.*, 1997). In this article, we report the crystal structure of the 2:1 side-by-side distamycin complex with an alternating DNA octamer containing only natural bases [d(GTATATAC)] and an extended TA stretch; this work has previously been reported in conferences (Mitra *et al.*, 1996, 1997).

2. Materials and methods

2.1. Synthesis and crystallization

The self-complementary DNA octamer d(GTATATAC) was synthesized by the solid-phase phosphoramidite method using an Applied Biosystems 381 DNA synthesizer. The DNA was cleaved from the column by 2 ml of 37% ammonium hydroxide and deprotected in a 328 K water bath overnight. The lyophilized sample was suspended in 25 µl of 2.5 *M* ammonium acetate and precipitated by 2 ml absolute ethanol at 248 K. The precipitate was isolated by centrifugation and further lyophilized before preparing stock solutions for crystallization. The drug–DNA complex was crystallized by the hanging-drop vapor-diffusion technique. The best crystals were obtained from a drop containing 1 m*M* DNA (single strand concentration), 20 m*M* sodium cacodylate buffer (pH 7.0), 1 m*M* distamycin A hydrochloride and 20 m*M* magnesium chloride equilibrated against 40% 2-methyl-2,4-pentanediol (MPD) in a reservoir at 293 K. Crystals appeared in a few days and grew to maximum dimensions of 0.25 × 0.25 × 0.60 mm.

2.2. Data collection and structure solution

A crystal measuring 0.25 × 0.25 × 0.60 mm was mounted in a thin-walled glass capillary with mother liquor at one end and sealed for intensity-data collection. Three-dimensional intensity data were collected on our Siemens–Nicolet area detector using Cu $K\alpha$ radiation from a MacScience rotating-anode

X-ray generator operating at 40 kV and 100 mA. A 0.3 mm collimator was used and the crystal-to-detector distance was 12.0 cm. The data were collected from one φ scan and two 0.25° width ω scans with an exposure time of 60 s per frame. The data were processed with the *XENGEN*2.1 software (Howard, 1990). In all, 3588 independent reflections ($F \geq 2\sigma$) were observed between 25.70 and 2.40 Å and the data completeness was 84.7%. The highest resolution bin, 2.51–2.40 Å, had 53.7% of the data.

The structure was solved by the molecular-replacement method using the program package *AMoRe* (Navaza, 1994). The cell volume indicated that the asymmetric unit probably contained two molecules of B-DNA with a volume per base pair of 1679 Å^3; known B-DNA structures have volume per base-pair ratios in the range 1100–1650 Å^3. The atomic coordinates of a related drug–DNA complex, distamycin–d(ICATATIC) (Chen *et al.*, 1997), without the distamycins, were used as the search model in the calculation of the rotation–translation function. The rotation search was performed using 3208 reflections between 8 and 2.5 Å and an integration radius of 12 Å. The top 15 peaks from the rotation search were used for the translation search and in the rigid-body refinement using the *FITTING* subroutine. The position of the second molecule was determined by an *n*-body (where $n \leq 4$ molecules in the asymmetric unit) translation search, as implemented in *AMoRe* (Navaza, 1994), keeping the first position fixed. A rigid-body refinement, using *FITTING* for the two positions yielded a correlation coefficient of 72.7% and an *R* index of 45.8%. Packing considerations reinforced the correctness of the structure.

Table 1
Crystal data and refinement statistics for the two independent d(GTATATAC)$_2$–distamycin molecules.

Crystal data	
Crystal system	Monoclinic
Space group	$P2_1$
Unit-cell parameters	
a (Å)	29.55
b (Å)	42.18
c (Å)	43.38
β (°)	96.56
Asymmetric unit	2 octamer duplexes + 4 distamycin A
Volume per base pair (Å^3)	1679
Resolution (Å)	2.40
Number of unique reflections	3588
Data completeness (%)	84.7
R_{sym} (%)	7.0

Refinement statistics	
Resolution range used (Å)	8-2.40
Number of reflections used	3467 ($\geq 2\sigma$)
Number of water molecules	55
R (%)	21.0
R_{free} (%)	28.6
R.m.s. deviation from ideal geometry	
Parameter file	param_nd.dna
Bond length (Å)	0.004
Bond angle (°)	1.09
Dihedral angle (°)	17.3

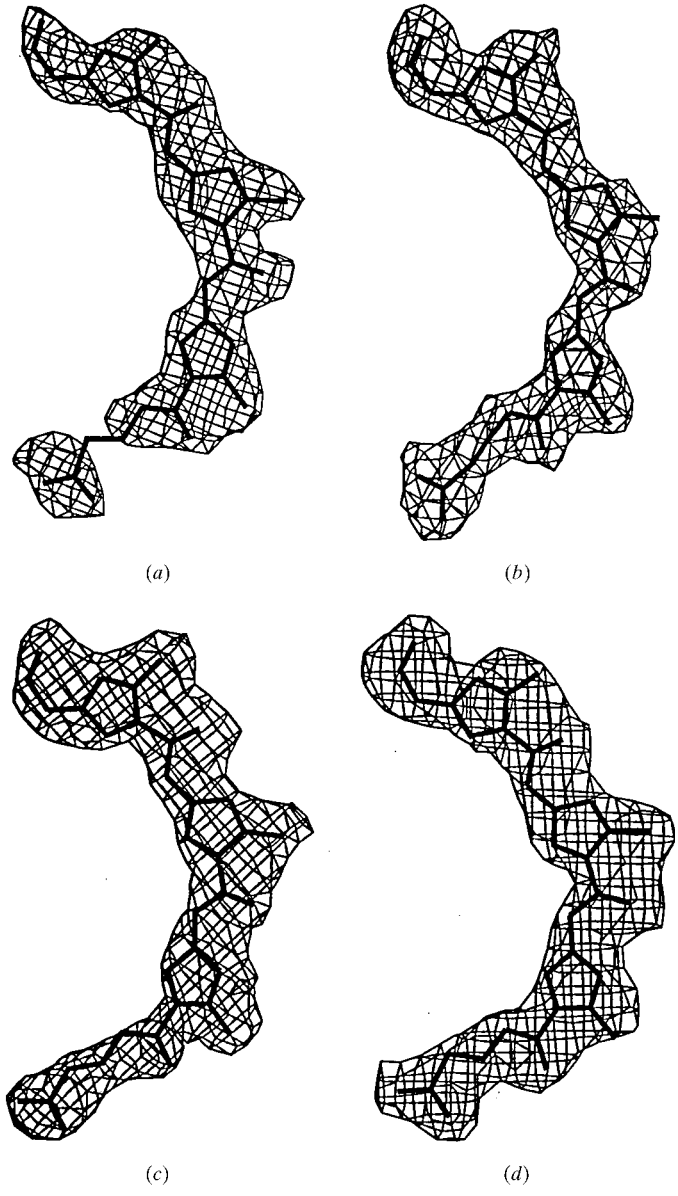

Figure 2
Final omit $|F_o| - |F_c|$ electron-density maps (contoured at 2.0σ) of the four distamycin molecules superimposed on their final coordinates. (*a*) A1, (*b*) A2, (*c*) B1 and (*d*) B2.

2.3. Refinement

The trial structure was refined using *X-PLOR* (Brünger, 1992). The structure refinement was monitored by calculating R_{free} with 10% of the reflections (Kleywegt & Brünger, 1996). A few cycles of rigid-body refinement using data between 8 and 2.40 Å and treating the duplexes as rigid units, brought the R_{index} down to 0.42 and R_{free} to 0.46. A round of positional refinement gave an R_{index} and R_{free} of 0.34 and 0.40, respectively. The correct bases [d(GTATATAC)] were assigned from the omit $|F_o| - |F_c|$ maps, and positional refinement gave an R_{index} and R_{free} of 0.33 and 0.38, respectively. A $2|F_o| - |F_c|$

map clearly showed the densities for the side-by-side binding of distamycin molecules in the minor groove of DNA. However, the distamycin molecules were not included in the refinement at this stage. A simulated-annealing refinement was performed by heating the system to 3000 K and slowly cooling to room temperature (300 K) with intervals of 0.5 fs (Brünger, 1988). The $R_{\rm index}$ and $R_{\rm free}$ dropped to 0.29 and 0.34, respectively. At various steps of the refinement 51 water molecules were added. Only those water peaks close to 3σ in the $|F_o| - |F_c|$ electron-density map and 1σ in the $2|F_o| - |F_c|$ map and at hydrogen-bonding distance ($\leq$3.4 Å) to DNA atoms were considered. The water molecules were assigned initial B factors of 40 Å^2 and positional refinement gave an $R_{\rm index}$ and $R_{\rm free}$ of 0.26 and 0.32, respectively. At this point, the four independent distamycin molecules in the two duplexes were fitted into the difference electron-density maps and their positions and B factors were refined to an $R_{\rm index}$ and $R_{\rm free}$ of 0.22 and 0.29, respectively. Strings of water molecules were also tried for the side-by-side distamycins which gave large residual electron densities and the $R_{\rm index}$ and $R_{\rm free}$ were also much higher (0.25 and 0.31, respectively), thereby confirming the presence of distamycins in the minor groove. An abnormally low temperature factor and a large residual difference electron density for one of the water molecules in the refinement indicated that it might be a metal ion. A sodium ion satisfied the electron density at this site, which was surrounded by a tetrahedral arrangement of four water molecules. Further cycles of positional and B-factor refinement gave a final $R_{\rm index}$ and $R_{\rm free}$ of 21.0 and 28.6%, respectively. The average B factors for the DNA atoms, distamycin A molecules and the solvent water were 21.8, 22.0 and 38.7 Å^2, respectively. The asymmetric unit consists of two independent octamer duplexes, four distamycin molecules, a sodium ion and 55 water molecules. Table 1 summarizes the crystal data and the refinement statistics for the structure.

Figs. 2(*a*)–2(*d*) show omit $|F_o| - |F_c|$ electron-density maps (contoured at 2.0σ) associated with the four independent distamycin A molecules. The root-mean-square deviations of bond lengths and bond angles from the ideal values are 0.004 Å and 1.09°, respectively. The coordinates and structure factors have been deposited with the NDB (Berman *et al.*, 1992; accession code GDH060).

3. Results and discussion

The 2:1 complex crystallizes with two independent DNA octamer molecules (*A* and *B*) in the asymmetric unit with side-by-side binding of distamycins A1 and A2 (molecule *A*) and B1 and B2 (molecule *B*) in the minor groove. Both DNA molecules are similar; the r.m.s. deviation on superposition is 0.43 Å. A stereoview of the DNA octamer (molecule *A*) with the bound distamycins is shown in Fig. 3. The 5′-terminal G–C pair does not interact with the drug. This monoclinic $P2_1$ complex contains two independent molecules in the asymmetric unit without an internal dyad. In contrast, the asymmetric unit of both the inosine side-by-side complexes in the tetragonal $P4_122$ space group (Chen *et al.*, 1994, 1995) and the monoclinic $C2$ side-by-side IC/AT octamer complexes (Chen *et al.*, 1997) contain only one DNA strand and one drug.

3.1. Conformation of the DNA octamers

The alternating octamer d(GTATATAC) with a purine start crystallizes as B-DNA, probably owing to drug binding (Chen *et al.*, 1995). Molecule *A* has 10.1 residues per turn while molecule *B* has 10.3 residues per turn, which is close to the non-integral number (10.3 to 10.6) observed in nucleosomal DNA (Wang, 1979; Rhodes & Klug, 1980; Wing *et al.*, 1980). The helical parameters were calculated using the *NEWHEL*92 program (Fratini *et al.*, 1982; Table 2). All the backbone torsion angles O5′—P (α) and C4′—C5′ (γ) are in the preferred g^-g^+ conformation, except T6 (molecule *A*) and C8 (molecule *B*), which were initially built with the next-preferred *tt* (*trans–trans*) conformation, but were changed on refinement to the least preferred g^+g^- (*gauche*$^+$–*gauche*$^-$) conformation (Yathindra & Sundaralingam, 1976). The helical twist angles for both molecules exhibit a regular alternation (averages 26.6 and 42.5°) with the purine–pyrimidine steps under-wound and the pyrimidine–purine steps over-wound, as found in similar alternating AT structures (Klug *et al.*, 1979; Yoon *et al.*, 1988). In Z-DNA, starting with either the 5′-pyrimidine (Wang *et al.*,

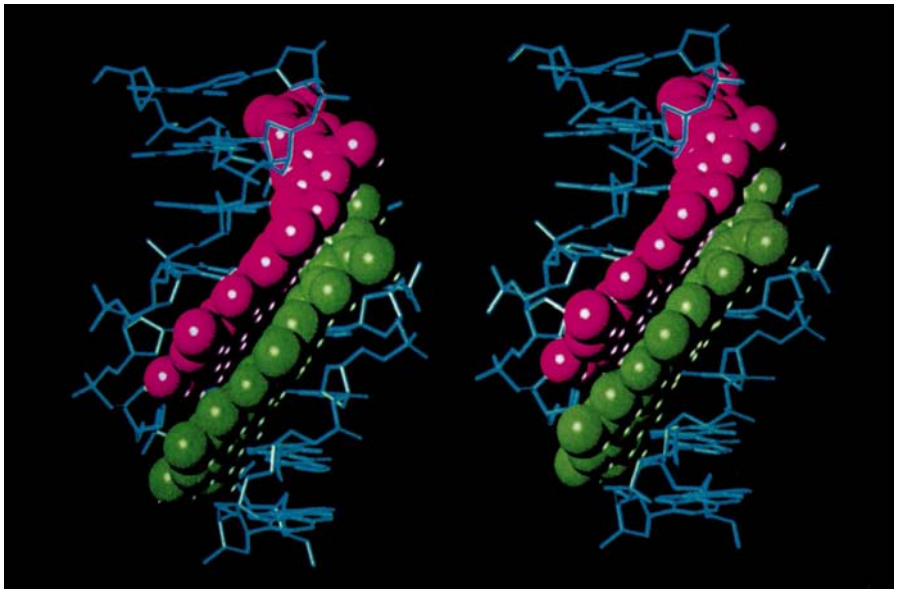

Figure 3
Stereo diagram of the d(GTATATAC)–distamycin complex (molecule *A*); molecule *B* is similar. Color coding: DNA, cyan; two distamycin drugs, purple and green. Note that the terminal G–C/C–G base pairs do not interact with the distamycins.

1979) or the 5′-purine (Ban *et al.*, 1996), the reverse situation is observed: the pyrimidine–purine steps are under-wound and the purine–pyrimidine steps are over-wound. The base-stacking distances are correlated to the twist angles; the low twist angles, *e.g.* C16–G1/A15–T2 and T14–A3/A13–T4, increase the intrastrand base stacking while the high twist angles A13–T4/T12–A5 decrease the intrastrand base stacking (Fig. 4). The twist angle increases to 47° at the middle of the duplex in molecule *A* and tapers off at the termini. Similarly, the roll angle is −19° in the middle of the helices and falls off at their termini. Also, in molecule *B* the twist (49°) and roll values (−15°) peak in the center and fall off at the termini (Table 2*b*). The central base pairs have higher inclinations and one of them is associated with high propeller twist. The torsion angles ε (C–O3′) and ζ (O3′–P) systematically alternate between tg^- and g^-t. These are referred to as B_I-DNA and B_{II}-DNA conformations, respectively. Also, the sugar puckering alternates between C2′-*endo* and C1′-*exo*.

3.2. Side-by-side *versus* 1:1 drug–DNA complexes

In both complexes, the distamycin molecules twist and turn to fit the curvature of the B-DNA minor groove. To accommodate two drugs in the 2:1 side-by-side complexes, the minor groove expands compared to that in the 1:1 single-drug complexes. The average width of the I–C/A–T segment expands to ∼7.7 Å in the side-by-side complexes (Chen *et al.*, 1994, 1995, 1997) compared to the average width of 4.1 Å in the 1:1 complexes. In the 1:1 binding mode, one strand is parallel to the drug and the other strand is antiparallel, and the drug interacts with both strands. In the side-by-side complexes the proximal DNA strand is parallel to each drug. (Note that the CONH groups of the drugs are parallel to the 5′→3′ direction of the DNA.) In the side-by-side complexes, dipole–dipole interactions and π–π interaction between the *N*-methyl pyrrole ring and the peptide group stabilize the drugs (Chen *et al.*, 1997). The drugs are 3.3 Å apart and stack with the

Table 2
Torsion angles (°) and helical parameters.

(*a*) The six torsion angles of the backbone, the base sugar glycosyl bond and the sugar pseudorotation

Molecule *A*

Residue	α	β	γ	δ	ε	ζ	χ	*P*
G1			171	149	168	265	247	170
T2	284	203	54	151	240	186	265	161
A3	296	153	44	142	191	259	263	172
T4	298	171	44	135	252	167	261	146
A5	290	135	54	139	187	260	261	166
T6	34	188	297	143	196	250	261	170
A7	319	151	49	137	199	244	257	150
C8	304	163	46	136			265	145
G9			62	146	185	261	234	168
T10	291	183	58	147	242	184	253	156
A11	298	152	35	142	182	274	154	177
T12	292	192	34	144	259	154	276	154
A13	292	144	42	143	171	269	265	172
T14	302	192	39	136	182	248	164	156
A15	322	166	54	131	169	281	261	148
C16	287	198	43	108			266	127
Average (sd)	291 (71)	171 (22)	71 (69)	139 (10)	202 (32)	236 (43)	260 (10)	158 (13)

Molecule *B*

Residue	α	β	γ	δ	ε	ζ	χ	*P*
G1			183	145	185	260	245	161
T2	293	185	47	144	241	180	262	155
A3	305	144	40	140	186	268	251	164
T4	300	187	32	144	249	158	281	155
A5	298	141	46	145	180	263	269	177
T6	304	173	48	131	196	235	260	143
A7	321	156	44	131	192	246	154	145
C8	28	180	306	152			261	167
G9			290	145	172	267	245	169
T10	290	197	49	147	223	192	254	155
A11	302	157	46	145	188	271	250	173
T12	297	182	37	138	242	161	272	150
A13	301	136	50	144	179	269	268	173
14	307	185	34	136	184	232	272	151
A15	327	153	50	135	195	256	253	152
C16	300	172	43	139			266	149
Average (sd)	283 (74)	168 (20)	84 (91)	141 (6)	201 (26)	233 (42)	260 (11)	159 (11)

Table 2 (continued)

(*b*) Helical parameters of molecule *A* and molecule *B*

Molecule *A*

Residue	Twist	Roll	Rise	Inclination	Propeller twist
G				2	−3
	26	0	3.8		
T				6	−10
	39	−3	3.5		
A				4	−8
	29	4	3.7		
T				6	−6
	47	−19	2.8		
A				4	−10
	26	−4	3.9		
T				4	−10
	39	0	3.3		
A				4	−5
	27	−3	3.9		
C				1	5

Molecule *B*

Residue	Twist	Roll	Rise	Inclination	Propeller twist
G				2	−1
	28	2	3.9		
T				5	−6
	40	2	3.2		
A				5	−11
	26	−2	3.8		
T				9	−16
	49	−15	3.0		
A				9	−9
	25	0	3.8		
T				5	−11
	40	2	3.4		
A				4	−4
	26	0	3.8		
C				2	4

N-methyl pyrrole ring of one with the peptide (CONH) group of the other, giving six pyrrole–peptide stacks (Fig. 5). Each drug spans about five base pairs and is sandwiched by the sugar–phosphate backbone on one side and the second drug on the other. The stacking of the two distamycin molecules is staggered and covers the entire octamer length, with the exception of the terminal base pairs.

Apart from the sandwiching van der Waals interactions mentioned above, the stability of the complex is maintained by the hydrogen-bonding interaction between the drugs and the DNA bases (Fig. 6). The four peptide NH groups of the drugs are involved alternately in hydrogen bonding to the purine base N3 and the pyrimidine base O2 of the proximal DNA strand. In contrast, in 1:1 complexes bifurcated hydrogen bonds are formed between adenine N3 and cytosine O2 on opposite strands. The propylamidinium tail of the drug is also hydrogen bonded to O2 of cytosine of the distal strand. The σ lone-pair orbitals of the backbone sugar O4′ are 3.2–3.5 Å distant from the π-electron clouds of their nearest *N*-methyl pyrrole rings. Even though the sugar O4′ atoms are at hydrogen-bonding distances from the peptide NH groups of the drugs, their N—H···O4′ angles (average 78°) are not

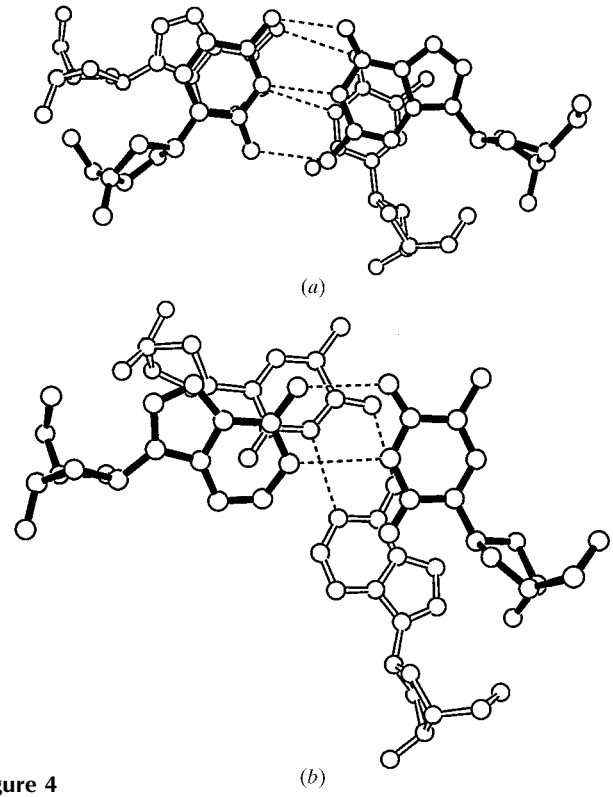

Figure 4
Base stacking at (*a*) low-twist step of C16–G1 (thick lines)/A15–T2 (open lines) and at (*b*) high-twist step of A13–T4 (thick lines)/T12–A5 (open lines).

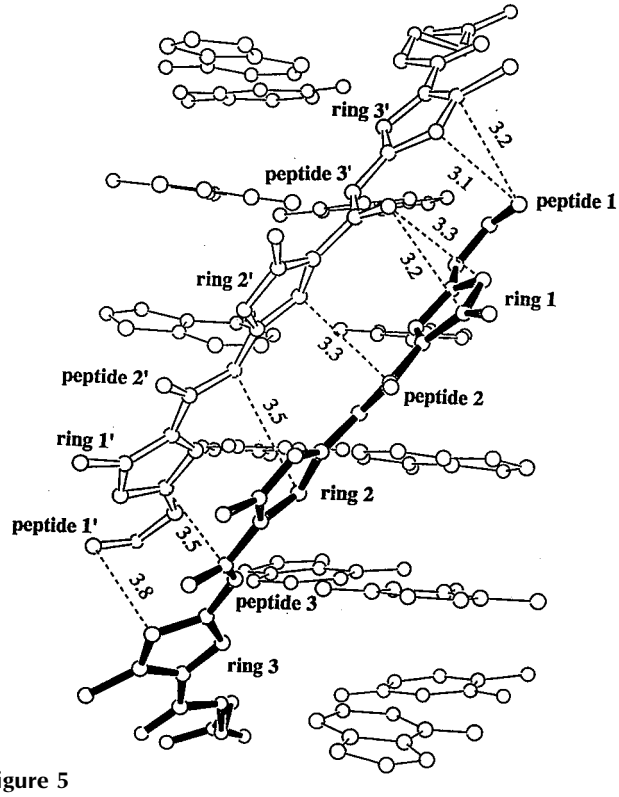

Figure 5
End-on view of the pyrrole/carboxamide stacking interactions of the two distamycin molecules. Short contacts (Å) are indicated by broken lines. Thick line, distamycin A1; open line, distamycin A2. The bases involved in hydrogen-bonding interactions with the distamycin molecules are also shown. Similar interactions are observed in molecule *B*.

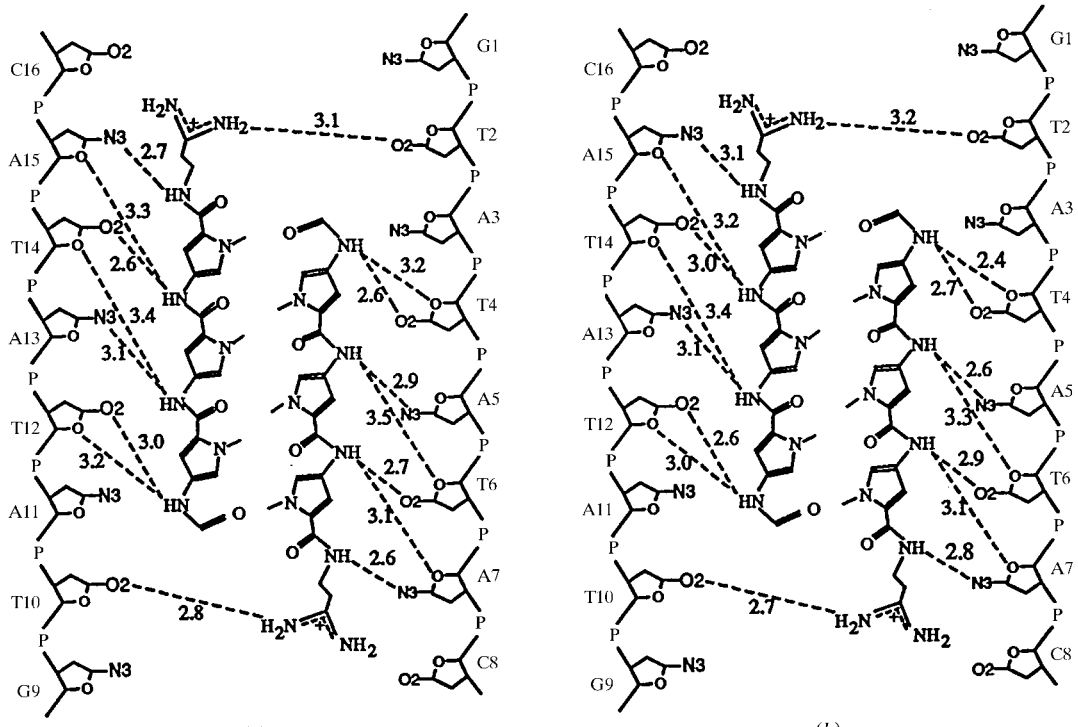

Figure 6
Hydrogen bonding for the drug–DNA complexes in (*a*) molecule *A*, (*b*) molecule *B*. The short contacts (not hydrogen bonded; see text) involving the O4′ of the sugars with the NH groups of the distamycins are also shown.

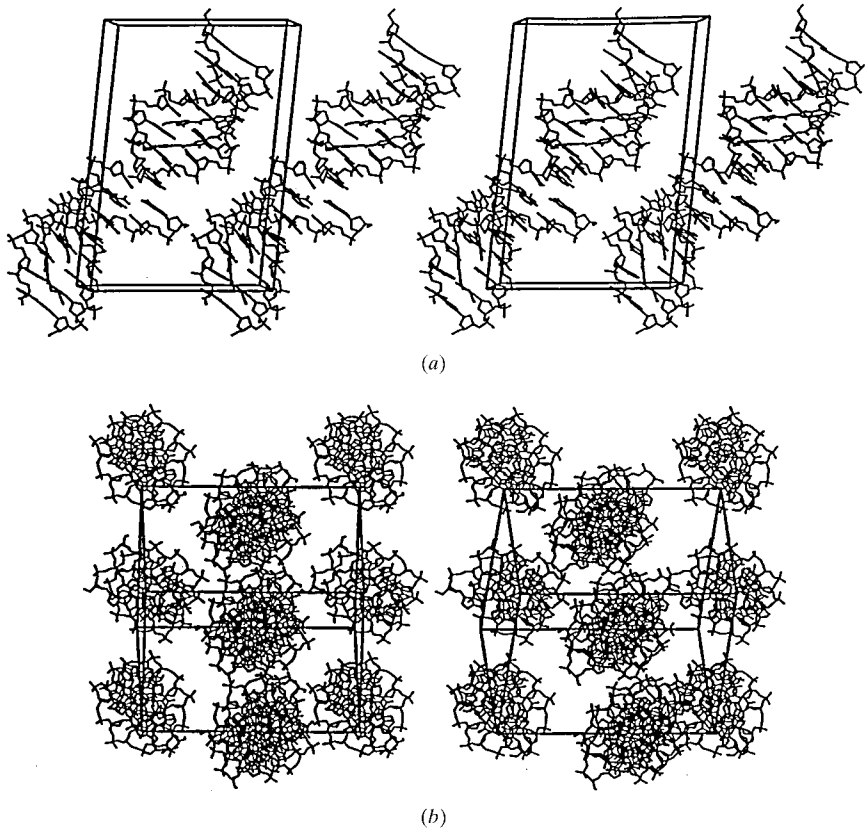

Figure 7
Stereo diagrams of crystal packing in the d(GTATATAC)–distamycin complex. (*a*) Stacking of the molecules parallel to the *ac* diagonal. The origin is at the top left-hand corner, the *a* axis is from the left to the right, the *b* axis is away from the plane of the paper towards the viewer and the *c* axis is from top to bottom. (*b*) The pseudo-hexagonal packing of the molecules. The origin is at the bottom left-hand corner, the *a* axis is vertically up, the *b* axis is from left to right and the *c* axis is from the bottom to the top inclined to the *a* axis.

pointed in the forward direction for hydrogen bonds (Jeffrey & Saenger, 1991) and hence cannot be properly described as hydrogen bonds.

3.3. Crystal packing and hydration

The crystal packing is shown in Fig. 7. The volume per base-pair ratio of 1679 Å^3 indicates that the molecules are not as tightly packed as in other 2:1 distamycin complexes, in which the volume per base-pair ratio is 1280–1425 Å^3 (Chen *et al.*, 1994, 1995, 1997). The octamer duplexes are stacked on top of each other to form pseudo-continuous helical columns displaced by 5.8 Å from the *ac* diagonal of the unit cell (Fig. 7*a*). The global helix axis of molecule A and molecule B are inclined to each other at an angle of 19°. The helical columns of the 2_1 screw-related molecules do not interact laterally. Each column of helices is surrounded by six neighboring columns in a pseudo-hexagonal packing arrangement (Fig. 7*b*); the 2_1 screw-related columns are 22.1 Å apart and the translation-related columns are 25.1 Å apart. A hydrated sodium ion bridges the screw-related columns. In all, 55 water molecules have been found, and the main hydration involves the major groove and the backbone phosphate atoms. The minor groove of the complex is not heavily hydrated because of the presence of the distamycins.

This work was supported by a NIH grant GM-17378 and an Ohio Eminent Scholar Endowment. Financial support by the University for the purchase of the Siemens Area Detector System is gratefully acknowledged.

References

Balendiran, K., Rao, S. T., Sekharudu, C. Y., Zon, G. & Sundaralingam, M. (1995). *Acta Cryst.* D**51**, 190–198.

Balendiran, K. & Sundaralingam, M. (1991). *Int. J. Quantum Chem. Quantum Biol. Symp.* **18**, 199–203.

Ban, C., Ramakrishnan, B. & Sundaralingam, M. (1996). *Biophys. J.* **71**, 1215–1221.

Berman, H. M., Olson, W. K., Beveridge, D. L., Westbrook, J., Gelbin, A., Demeny, T., Hsieh, S. H., Srinivasan, A. R. & Schneider, B. (1992). *Biophys. J.* **63**, 751–759.

Brünger, A. T. (1988). *Crystallographic Refinement by Simulated Annealing. Crystallographic Computing 4: Techniques and New Technologies*, edited by N. W. Isaacs & M. R. Taylor, pp. 126–140. Oxford: Clarendon Press.

Brünger, A. T. (1992). *X-PLOR Manual Version 3.0*. Yale University, New Haven.

Burckhardt, G., Luck, G., Zimmer, C., Storl, J., Krowicki, K. & Lown, J. W. (1989). *Biochem. Biophys. Acta*, **1009**, 11–18.

Chen, X., Ramakrishnan, B., Rao, S. T. & Sundaralingam, M. (1994). *Nature Struct. Biol.* **1**, 169–175.

Chen, X., Ramakrishnan, B. & Sundaralingam, M. (1995). *Nature Struct. Biol.* **2**,733–735.

Chen, X., Ramakrishnan, B. & Sundaralingam, M. (1997). *J. Mol. Biol.* **267**, 1157–1170.

Coll, M., Frederick, C. A., Wang, A. H.-J. & Rich, A. (1987). *Proc. Natl Acad. Sci. USA*, **84**, 8385–8389.

Fratini, A. V., Kopka, M. L., Drew, H. R. & Dickerson, R. E. (1982). *J. Biol. Chem.* **257**, 14686–14707.

Geierstanger, B. H., Mrksich, M., Dervan, P. B. & Wemmer, D. E. (1994). *Science*, **266**, 646–650.

Geierstanger, B. H. & Wemmer, D. E. (1995). *Annu. Rev. Biophys. Biomol. Struct.* **24**, 463–493.

Goodsell, D. S., Ng, H. L., Kopka, M. L., Lown, J. W. & Dickerson, R. E. (1995). *Biochemistry*, **34**, 16654–16661.

Howard, A. J. (1990). *XENGEN 2.1 Manual.* Genex Corporation, Gaitherburg, MD.

Jeffrey, G. A. & Saenger, W. (1991). *Hydrogen Bonding in Biological Structures.* Berlin: Springer–Verlag.

Kielkopf, C. L., Baird, E. E., Dervan, P. B. & Rees, D. C. (1998). *Nature Struct. Biol.* **5**, 104–109.

Kleywegt, G. J. & Brünger, A. T. (1996). *Structure*, **4**, 897–904.

Klug, A., Jack, A., Viswamitra, M. A., Kennard, O., Shakked, Z. & Steitz, T. A. (1979). *J. Mol. Biol.* **131**, 669–680.

Kopka, M. L., Goodsell, D., Han, G. W., Chiu, T. K., Lown, J. W. & Dickerson, R. E. (1997). *Structure*, **5**, 1033–1046.

Kopka, M. L. & Larsen, T. A. (1992). *Nucleic Acid Targeted Drug Design*, edited by C. L. Props & T. J. Perun, pp. 303–374. New York: Marcel Dekker.

Kopka, M. L., Yoon, C., Goodsell, D., Pjura, P. & Dickerson, R. E. (1985*a*). *J. Mol. Biol.* **183**, 553–563.

Kopka, M. L., Yoon, C., Goodsell, D., Pjura, P. & Dickerson, R. E. (1985*b*). *Proc. Natl Acad. Sci. USA*, **82**, 1376–1380.

Lown, J. W., Krowicki, K., Balzarini, J. & De Clercq, E. (1986). *J. Med. Chem.* **29**, 1210–1214.

Mitra, S. N., Wahl, M. C., Chen, X. & Sundaralingam, M. (1996). Abstract P-12, 54th Annual Pittsburgh Diffraction Conference.

Mitra, S. N., Wahl, M. C. & Sundaralingam, M. (1997). *J. Biomol. Struct. Dyn.* **14**, 875.

Mrksich, M. & Dervan, P. B. (1993). *J. Am. Chem. Soc.* **115**, 9892–9897.

Navaza, J. (1994). *Acta Cryst.* A**50**, 157–160.

Patel, D. J. & Shapiro, L. (1985). *Biochimie*, **67**, 887–915.

Pelton, J. G. & Wemmer, D. E. (1989). *Proc. Natl Acad. Sci. USA*, **86**, 5723–5727.

Portugal, J. & Waring, M. J. (1987). *Eur. J. Biochem.* **167**, 281–289.

Rhodes, D. & Klug, A. (1980). *Nature (London)*, **286**, 573–578.

Wahnert, U., Zimmer, O., Luck, G. & Pitra, O. (1975). *Nucleic Acids Res.* **2**, 391–404.

Wang, A. H.-J., Quigley, G. L., Kolpak, F. J., Crawford, J. L., Van Boom, J. H., Van der Marel, G. & Rich, A. (1979). *Nature (London)*, **282**, 680–686.

Wang, A. H.-J. & Teng, M. (1990). *Crystallographic and Modeling Methods in Molecular Design*, edited by C. E. Bugg & S. E. Ealick, pp. 123–150. New York: Springer–Verlag.

Wang, J. C. (1979). *Proc. Natl Acad. Sci. USA*, **76**, 200–203.

Wartell, R. M., Larson, J. E. & Wells, R. D. (1974). *J. Biol. Chem.* **249**, 6719–6731.

White, S., Baird, E. E. & Dervan, P. B. (1997). *Chem. Biol.* **4**, 569–578.

White, S., Szewczyk, J. W., Turner, J. M., Baird, E. E. & Dervan, P. B. (1998). *Nature (London)*, **391**, 468–471.

Wing, R., Drew, H., Takano, T., Broka, C., Tanaka, S., Itakura, K. & Dickerson, R. E. (1980). *Nature (London)*, **287**, 755–758.

Yathindra, N. & Sundaralingam, M. (1976). *Nucleic Acids Res.* **3**, 729–747.

Yoon, C., Prive, G. G., Goodsell, D. S., Dickerson, R. E. (1988). *Proc. Natl Acad. Sci. USA*, **85**, 6332–6336.

Zakrzewska, K., Lavery, R. & Pullman, B. (1983). *Nucleic Acids Res.* **11**, 8825–8839.

Zimmer, C. & Wahnert, U. (1986). *Prog. Biophys. Mol. Biol.* **47**, 31–112.